60-GHz MONOLITHIC OSCILLATOR USING InGaP/InGaAs/GaAs HEMT TECHNOLOGY

Yoshihiro Kawasaki, Kazuo Shirakawa, Yoji Ohashi and *Tamio Saito
Fujitsu Laboratories Ltd.

*Advanced Millimeter Wave Technologies, Co., Ltd.
1015 Kamikodanaka, Nakahara-ku, Kawasaki 211, Japan
E-mail: yosihiro@flab.fujitsu.co.jp

Abstract

Using 0.11-μm InGaP/InGaAs/GaAs pseudomorphic HEMT technology, we have developed a 60-GHz buffered free-running monolithic oscillator which has an output power of 9.1 dBm at 59.7 GHz and a phase noise of -60 dBc/Hz at 100 kHz from the carrier frequency. We operated the oscillator's HEMT in a reverse channel configuration and introduced an empirical nonlinear HEMT model for the configuration.

Introduction

InP-based HEMT devices are considered preferable for millimeter wave oscillators [1]. However, they are not sufficiently reliable at present. Also, their fabrication process is incompatible with that of GaAs-based HEMTs. InGaP/InGaAs/GaAs pseudomorphic HEMTs can be the best GaAs-based HEMTs and are suitable for use in millimeter wave oscillators. InGaP/InGaAs/GaAs pseudomorphic HEMTs have better noise and gain performance than AlGaAs/InGaAs/GaAs pseudomorphic HEMTs due to their thinner electron supply layer (InGaP) and better carrier confinement in the pseudomorphic quantum-well channel [2]. Using InGaP/InGaAs/GaAs HEMTs, we designed and fabricated a 60-GHz oscillator followed by a buffer amplifier. To generate enough negative resistance and reduce circuit size, we adopted the reverse channel HEMT configuration [3][4].

The oscillator is intended for use in 60-GHz band commercial systems such as automotive collision warning systems (FM-CW-based radar systems).

Reverse channel configuration and HEMT model

We used passivated HEMTs having two T-shaped gate fingers each measuring 0.11 by 50 μm. Their drain current was typically -30 mA and a DC transconductance of 42 mS at a V_{ds} and a V_{gs} of -3 V. When the HEMT is operated in the reverse channel configuration, C_{gd} becomes greater than C_{gs}, and consequently it acts as an internal gate-to-drain feedback circuit. The internal drain current source is controlled by the intrinsic voltage across Cgd. When the reverse channel operation is applied to the common two-ports reflection-type oscillator's HEMT, the required source-to-ground feedback circuit becomes inductive, and can be easily achieved using less than a quarter wavelength short-ended line. The parasitic source inductance and via holes inductance are also regenerated as feedback elements. By using the reverse channel configuration, adequate negative resistance can be easily generated with simple feedback circuits.

The equivalent circuit of the HEMT in reverse channel configuration is shown in Figure 1. The main nonlinear elements are C_{gd} and the drain current source. The model was based on S-parameters measured up to 62.5 GHz under various bias conditions. The extrinsic elements (L_g, R_g, L_d, R_d, L_s and R_s) were determined by finding a value which minimizes the frequency dependence of all intrinsic nonlinear elements [5]. All nonlinear elements and the drain current source in the model were defined using original equations. In the reverse channel configuration HEMT, the C_{gd}-V_{gd} and C_{gs}-V_{gd} characteristics are similar to the C_{gs}-V_{gs} and C_{gd}-V_{gs} characteristics for the common source configuration HEMT respectively. Utilizing these similarities, we expressed Cgs and Cgd in the reverse channel configuration HEMT, by using the same formulas as those for Cgd and Cgs in the common source configuration HEMT respectively. By comparing the S-parameters of the model with the measured S-parameters under various bias conditions, we verified the model. Figure 2 shows the comparison of results for a V_{ds} and V_{gs} of -3 V, which is the adopted DC bias point for the oscillator's HEMT.

Oscillator design

Figure 3 illustrates the oscillator circuit schematic. A short-ended 50-Ω microstripline (T1) is connected to the drain terminal of the HEMT. The line is bent and its other end is connected to an MIM capacitor on a via hole. The oscillation power is taken from the gate side of the HEMT.

For a T1, some given Γ_A (>1) may satisfy the oscillation start-up condition. And some of them might give the steady-stated oscillation at the desired frequency. We determined the Γ_A which would ensure steady-state oscillation at the desired frequency (60GHz for our design) for varied lengths of T1. Then, calculating the associated oscillation power and plotting them onto Smith charts, the design information for optimum output can be obtained. We designed our oscillator based on this approach. To operate with an output power of +7.2 dBm at 60 GHz, we set Γ_A to point B in Figure 4. At this point, the magnitude of $\Gamma_A * \Gamma_R$ is 1.5 and the oscillation start-up frequency is 60.4 GHz.

A buffer amplifier was designed together with the oscillator. The HEMT used in the amplifier is the same type as that in the oscillator, but operates in a common source configuration.

Oscillator performance

Figure 5 shows a photo of the buffered oscillator. Figure 6 displays the buffered oscillator's output spectrum. Figures 7 and 8 exhibit the frequency and power characteristics of the oscillator without the buffer amplifier stage. (An oscillator without an amplifier was also fabricated). The oscillation power is +6.7 dBm at 59.71 GHz for a V_{ds} of -3 V and a V_{gd} of 0 V. This was the adopted bias during the design. The DC-to-RF conversion efficiency is about 9 %. The oscillation frequency varies from 59.78 to 59.58 GHz as V_{gd} changes from -0.3 V to +0.5 V. Figure 8 demonstrates that the oscillator using the reverse channel configuration HEMT can be driven by only one DC source.

The oscillator with the buffer amplifier has an output power of 9.1 dBm at 59.7 GHz and at the same DC bias as that above (Figure 9). The oscillator's phase noise at 100 kHz from the carrier frequency is approximately -63 dBc/Hz and adding the amplifier increases it by 3 dB (Figure 10). As may be seen from Figures 7 and 9, the addition of the amplifier to the oscillator causes a small frequency shift of within 140 MHz. The oscillation frequency instantly changes within 400 kHz at room temperature(Figure 11). The buffered oscillator's maximum frequency shift caused by external load changes is 50 MHz, which is one fifth that of the oscillator without the amplifier.

Conclusion

Using 0.11-µm InGaP/InGaAs/GaAs pseudomorphic HEMT technology and operating the HEMT in a reverse channel configuration, we have developed a 60-GHz buffered monolithic oscillator which has an output power of 9.1 dBm at 59.7 GHz. The phase noise is -60 dBc/Hz at 100 kHz from the carrier frequency. This performance is good for millimeter wave free-running HEMT oscillators.

In this paper, we have demonstrated that InGaP/InGaAs/GaAs HEMTs can be used in millimeter wave oscillator devices. We are confident of successful further improvements such as the integration of a varactor diode and stabilization using a dielectric resonator.

The reverse channel configuration is rarely used, but it is certainly suitable for a millimeter wave oscillator. In our calculation, the oscillator using the reverse channel configuration HEMT and that using the common source configuration HEMT have little difference in RF performance. The problem in using reverse channel configuration lies in the insufficient study of nonlinear HEMT model for this configuration. We introduced an empirical nonlinear HEMT model describing the reverse channel operation, which is basically based on the common source configuration HEMT model. It was implemented in HP MDS with some convergence problem not fatal for the design. The continuation of the model study is required.

Reference

[1] Y. Kwon et al., "A D-band Monolithic Fundamental Oscillator using InP-based HEMT's," IEEE MW& MMW Circuit-S Digest, pp. 49-52, 1993.
[2] M. Takikawa and K.Joshin, "Pseudomorphic N-InGaP/InGaAs/GaAs High Electron Mobility Transistors for Low Noise Amplifiers," IEEE Electron Device Lett., vol. 14, pp. 406-408, 1993.
[3] G. Gonzalez, "Microwave Transistor Amplifiers Analysis and Design," Pentice-Hall Inc., 1984.
[4] F. S. Correra et al., "18GHz Reverse Channel HEMT Oscillator," IEEE MTT-S, pp. 423-426, 1990.
[5] K. Shirakawa et al., "An Approach to Determining an Equivalent Circuit for HEMTs," IEEE Trans. Microwave Theory Tech., May 1995 in press.

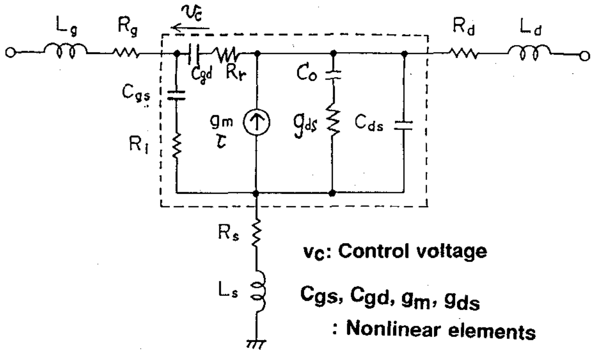

Fig. 1. HEMT equivalent circuit.

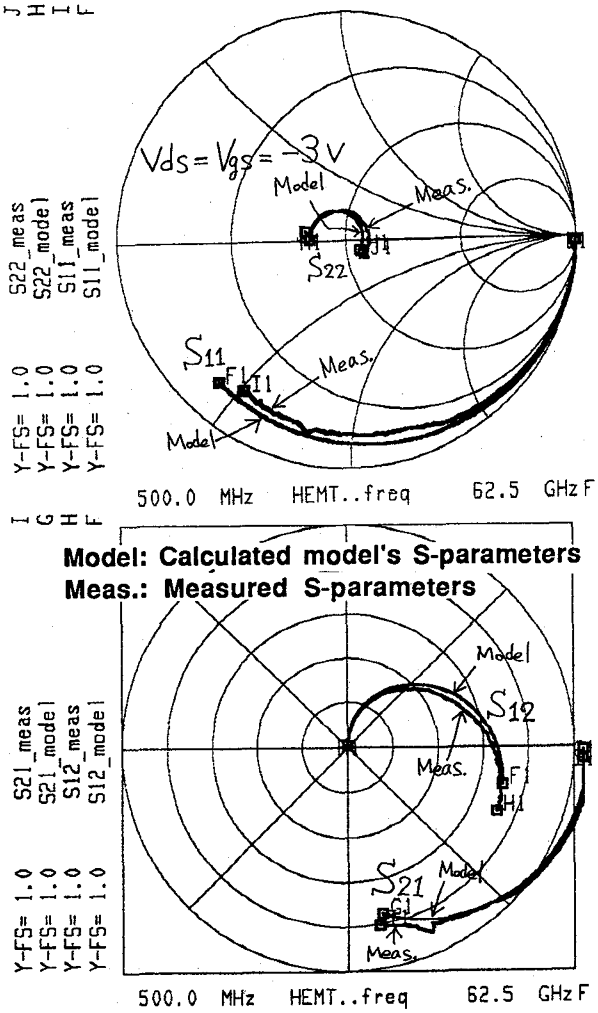

Fig. 2. S-parameters comparison.

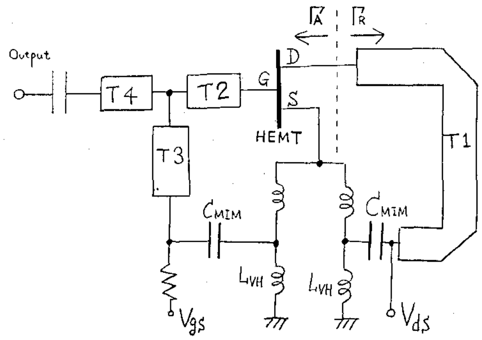

C_{MIM}: Capacitance of MIM capacitor
L_{VH}: Inductance of via hole
Γ_A, Γ_R: Reflection coefficients when oscillation starts

Fig. 3. Schematic of oscillator circuit.

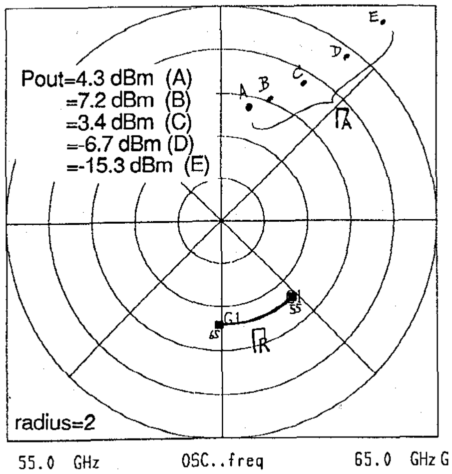

Fig. 4. Γ_A for 60-GHz steady-state oscillation.

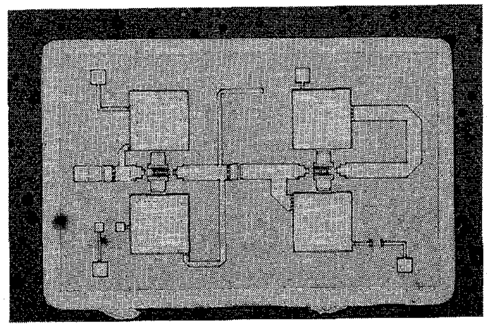

Chip size: 1.4 × 0.92 × 0.075 mm

Fig. 5. Photo of the buffered oscillator.

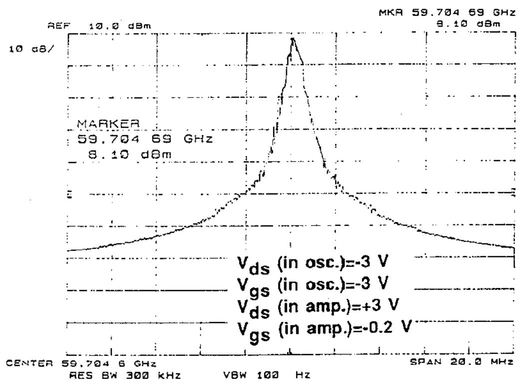

Fig. 6. Output spectrum of the buffered oscillator.

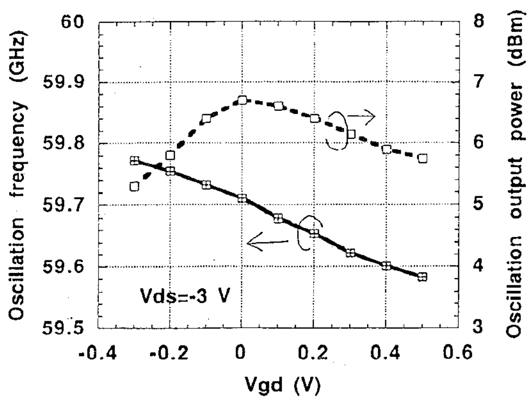

Fig. 7. Frequency and output power vs. Vgd characteristics of the oscillator without the buffer amplifier.

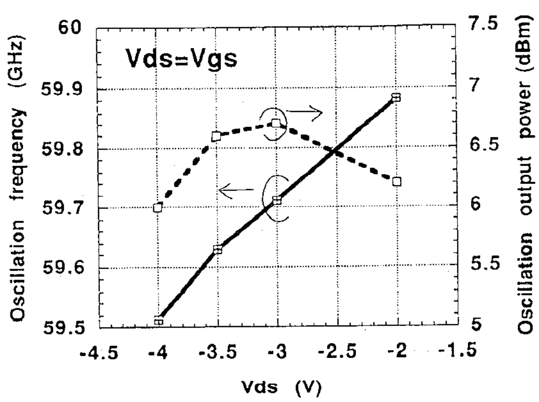

Fig. 8. Frequency and output power vs. Vds characteristics of the oscillator without the buffer amplifier.

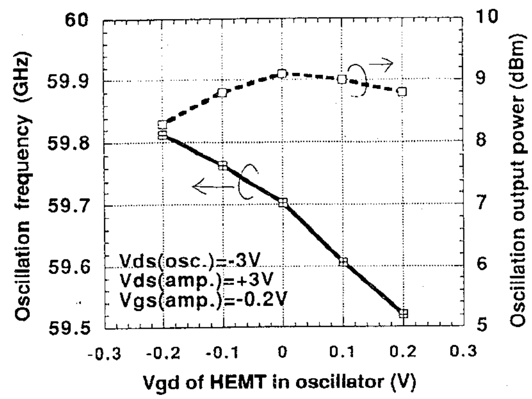

Fig. 9. Frequency and output power characteristics of the buffered oscillator.

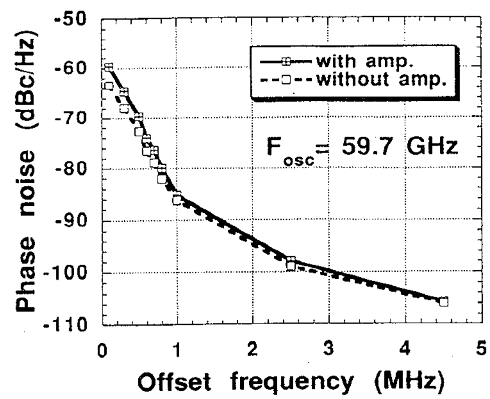

Fig. 10. Phase noise characteristics of the oscillator with and without the amplifier.

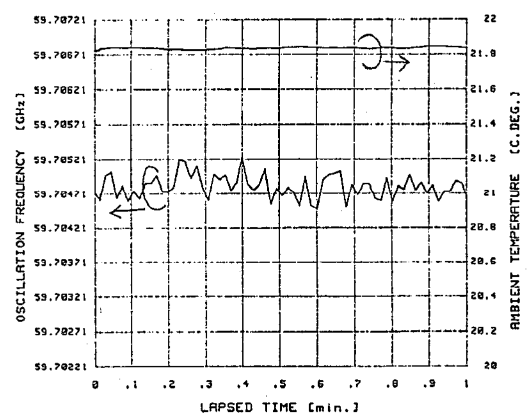

Fig. 11. Fluctuation of oscillation frequency in the buffered oscillator.